Automatic retinal vascularity identification and artery/vein classification using near-infrared reflectance retinographies

Joaquim de Moura[1,2], Jorge Novo[1,2], Marcos Ortega[1,2], Noelia Barreira[1,2], and Pablo Charlón[3]
{joaquim.demoura, jnovo, mortega, nbarreira}@udc.es, pcharlon@sgoc.es

[1] Department of Computer Science, University of A Coruña, A Coruña (Spain)
[2] CITIC - Research Center of Information and Communication Technologies, University of A Coruña, A Coruña (Spain)
[3] Instituto Oftalmológico Victoria de Rojas, A Coruña (Spain)

Abstract. The retinal microcirculation structure is commonly used as an important source of information in many medical specialities for the diagnosis of relevant diseases such as, for reference, hypertension, arteriosclerosis, or diabetes. Also, the evaluation of the cerebrovascular and cardiovascular disease progression could be performed through the identification of abnormal signs in the retinal vasculature architecture. Given that these alterations affect differently the artery and vein vascularities, a precise characterization of both blood vessel types is also crucial for the diagnosis and treatment of a significant variety of retinal and systemic pathologies. In this work, we present a fully automatic method for the retinal vessel identification and classification in arteries and veins using Optical Coherence Tomography scans. In our analysis, we used a dataset composed by 30 near-infrared reflectance retinography images from different patients, which were used to test and validate the proposed method. In particular, a total of 597 vessel segments were manually labelled by an expert clinician, being used as groundtruth for the validation process. As result, this methodology achieved a satisfactory performance in the complex issue of the retinal vessel tree identification and classification.

Keywords: Retinal imaging, vascular tree, segmentation, artery/vein classification

1 Introduction

The retina is the only tissue of the human body where the information of the vascular morphology and structure can be evaluated non-invasively and in vivo [1]. The retinal vasculature is a complex network of blood vessels composed of arteries, veins and capillaries [2]. In the current clinical practice, optical imaging

is widely used in the study, diagnosis, planning, and assessment of the treatment response in a variety of ocular and systemic diseases that affect the retinal vasculature as, for reference, hypertension [3], diabetes [4] or arteriosclerosis [5]. The most common symptoms of those pathologies include micro-aneurysms, vascular tortuosity, arteriovenous nicking or neovascularization.

In many studies, different biomarkers are used to measure the vascular morphology of the retina, particularly between arteries and veins. As reference, we can find the Arterio-Venular-Ratio (AVR) that is defined by the ratio between the arteriolar and the venular diameters [6]. In particular, this biomarker is used by the clinical specialists in the diagnosis of several pathologies as, for example, diabetic retinopathy, which is among the major causes of blindness worldwide [7]. Therefore, an accurate identification of the retinal vasculature structure and its characterization in arteries and veins is essential for the diagnosis and monitoring of the treatment of a variety of retinal pathologies [8].

Nowadays, Computer-Aided Diagnosis (CAD) systems are increasingly being used as auxiliary tools by the expert clinicians for the detection and interpretation of different diseases [9] [10] [11]. These independent decision systems are designed to assist clinicians in various tasks, including storage, retrieval, organization, interpretation, and diagnostic output of hypothetical pathological images and data [12], facilitating and simplifying their work.

Optical Coherence Tomography (OCT) is a non-invasive, cross-sectional and high-resolution image modality that allows the acquisition of three-dimensional images of the retinal tissues in real time [13]. This retinal imaging technique uses low-coherence interferometry to obtain a series of OCT histological sections by sequentially collecting reflections from the lateral and longitudinal scans of the ocular tissues of the human eye [14]. The OCT sections are complemented with the corresponding near-infrared reflectance (NIR) retinography image of the eye fundus. Both images are simultaneously captured with the same OCT capture device. Figure 1 shows a representative example of an OCT image composed by the NIR retinography image and a corresponding OCT histological section.

(a) (b)

Fig. 1. Example of OCT scan. (a) NIR retinography image. (b) OCT histological section.

Given the importance and applicability of the analysis of retinal images, many efforts were done to face the analysis with classical retinographies. Thus, as reference, in the work proposed by Joshi *et al.* [15], a methodology was designed to automatically segment the vascular tree structure using a strategy that is based on graph theory. Then, the blood vessel classification process into arteries and veins is done using properties of color spaces. Dashtbozorg *et al.* [16] proposed an automatic method for the artery/vein classification using a graph-based approach and different machine learning methods. Following a similar strategy, Yang *et al.* [17] proposed a method using a Support Vector Machine (SVM) classifier for the vessels categorization in retinal images. Kondermann *et al.* [18] proposed a method using SVM and Artificial Neural Networks (ANN) in a feature extraction and classification process. Relan *et al.* [19] proposed an unsupervised method of classification based on a Gaussian Mixture Model on small vessel patches to classify the main vessels structures. Welikala *et al.* [21] proposed an automatic methodology using a Convolutional Neural Network (CNN) approach for the automatic classification of arteries and veins in retinal images. The final architecture of this method was composed of six learned layers: three convolutional and three fully-connected. Similarly, Girard *et al.* [22] proposed a method for artery/vein classification combining CNN and graph propagation strategies. In the work of Huang *et al.* [23], the authors proposed a methodology using a set of features that are extracted from the lightness reflection of the blood vessels. Then, a Linear Discriminate Analysis (LDA) learning strategy was used to validate these selected features. In the work proposed by Zou *et al.* [24], a supervised classification method based on feature selection is done. Firstly, the grey-level co-occurrence matrix (GLCM) and adaptive local binary pattern (A-LBP) features are extracted. Then, a Feature-Weighted K-Nearest Neighbors (FW-KNN) algorithm is used to classify the arteries and veins vessels. In the work of Vázquez *et al.* [20], the authors proposed a framework for the automatic classification of the arteries and veins using a k-means clustering. Then, this information is used to calculate the AVR biomarker.

In this work, we present a fully computational method for the automatic extraction of the retinal vascular structure and its classification into arteries and veins using, only, the information that is obtained through the NIR retinography images. As we said before, these images are provided in combination with the histological sections of the OCT scans. For this purpose, the method extracts the retinal vessel tree and uses the k-means clustering algorithm with local features to differentiate the arteries from the veins. A post-processing stage is carried out using the anatomical knowledge of the vessels to identify and correct the possible misclassifications of the individual vessel points. Promising preliminary results of this method were obtained in the work proposed in [25]. In this context, this methodology was extended and further deeply validated in this work, expanding its potential for the identification and classification of arteries and veins in this image modality.

This work is organized as follows: Section 2 presents the proposed methodology and the characteristics of all the involved stages. Section 3 details all the

experiments that were done to validate the method as well as the discussion about the obtained results. Finally, Section 4 includes the conclusions of this proposal as well as the possible future lines of work.

2 Methodology

In this work, the system receives, as input, the NIR retinography image to identify and classify the vascular tree into arteries and veins. The proposed methodology is divided into three main stages: firstly, the entire retinal vascular tree is extracted from the input image; secondly, the region of the optic disc is identified and removed for the posterior analysis; and finally, the remaining identified vessels are analysed and classified into arteries and veins. Figure 2 describes the general scheme of the proposed methodology, from where each stage will be detailed in the following subsections.

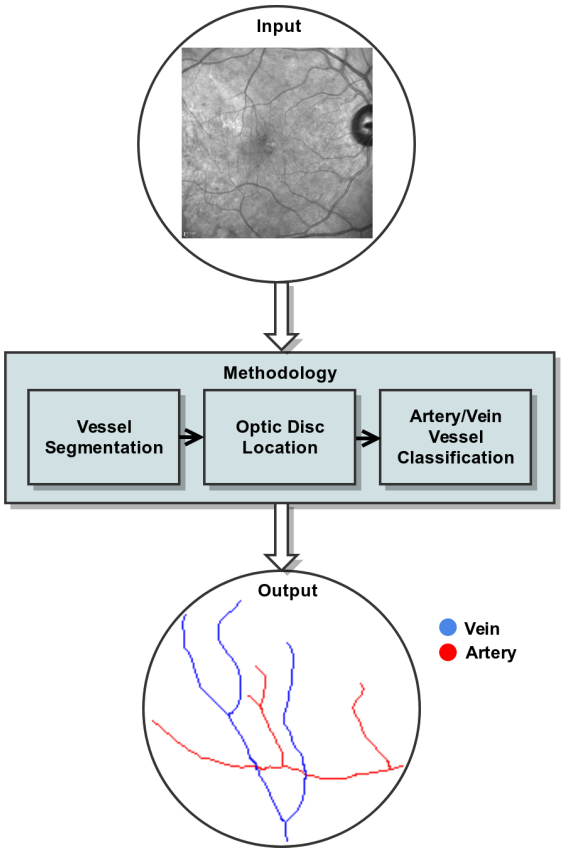

Fig. 2. Main stages of the proposed methodology.

2.1 Vessel Segmentation

The first stage of the classification process faces the segmentation of the retinal vessel tree within the NIR retinography image. For this purpose, we follow the method proposed by Calvo *et al.* [26], given its simplicity and for being a well-established and robust technique that demonstrated its suitability in classical retinographies.

Firstly, an initial segmentation was performed by means of a hysteresis-based thresholding strategy. To achieve this, a hard threshold (T_h) obtains pixels with a high confidence of being vessels while a weak threshold (T_w) keeps all the pixels of the vessel tree, including the spurious ones. The final segmentation is formed by all the pixels that were included by the T_w weak threshold connected to, at least, one pixel obtained by the T_h hard threshold. The values for T_h and T_w are extracted using as reference two metrics that are calculated on the NIR retinography images: the percentage of vascular tree and the percentage of background. These thresholds are calculated using the percentile values, according to Equation (1).

$$P_k = L_k + \frac{k(n/100) - F_k}{f_k} \times c, \quad k = 1, 2, ..., 99 \tag{1}$$

where L_k is the percentile lower limit k, n represents the size of the data set, F_k is the accumulated frequency for $k-1$ values, f_k depicts the frequency of percentile k and c is the measurement of the size of the percentile interval. In our case, c is equal to 1. A representative example of this stage of the vessel tree segmentation is presented in Figure 3.

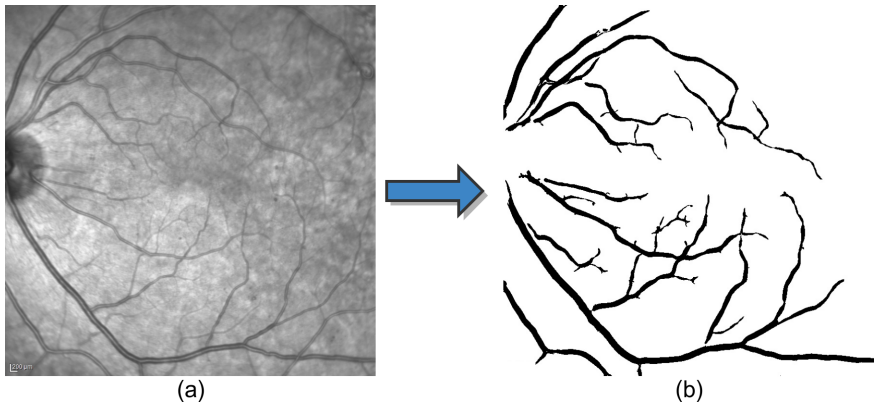

Fig. 3. Segmentation process of the retinal vessel tree. (a) Input NIR retinography image. (b) Vessel tree segmentation image.

Next, the vessel centerline is calculated to represent the vasculature as a list of representative segments using as baseline the information that was ob-

tained in the previous segmentation. For this purpose, the implemented strategy was based in the work of Caderno *et al.* [27], where the retinal segments are located by means of the Multi Local Set of Extrinsic Curvature enhanced by the Structure Tensor (MLSEC-ST) operator. The operator detects the tubular structures (ridges or valleys) by means of the analysis of the structure tensor of the segmentation image. And finally, a skeletonization process is done to obtain the representation of the vessel centerline of each vascular segment. Figure 4 presents an example with the result of the centerline identification process.

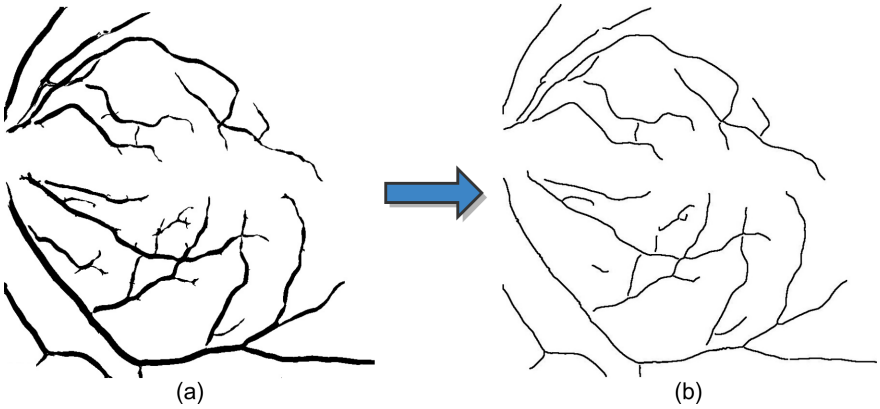

Fig. 4. Vessel centerline identification process of the retinal vessel tree. (a) Input vessel tree segmentation image. (b) Vessel tree centerline identification image.

2.2 Optic Disc Location

The optic disc is the region that presents the highest variation of intensities of adjacent pixels in comparison with the rest of the eye fundus. This scenario can disturb the characteristics of the visualization of the vascular structures, a situation that can lead to misclassifications of the surrounding vessel positions and, consequently, of the vessel segments. For that reason, the optic disc region is frequently excluded for the analysis of the retinal vessel tree, as is our case.

To achieve this, we implemented an algorithm based on the work proposed by Blanco *et al.* [28], given its simplicity and the satisfactory results that were obtained for this issue in classical retinographies. Firstly, two Gaussian filters were applied at different scales with a blob operator to identify a region of interest that contains the optic disc. Then, the edges are calculated using the Sobel edge detector [29]. Finally, we extract the optic disc region using the Fuzzy Circular Hough transform [30]. Figure 5(a) shows an example of the optic disc extraction, where r represents the radius of the located optic disc.

In many cases, not only the optic disc but also its contiguous region may include significant intensity changes, being this area of the image biased to bright intensities. As mentioned, this situation can lead to misclassifications of its containing vessels as arteries and veins in posterior stages of the method. To solve this problem, we remove a circular region centered on the optic disc with a radius of $1.5 \times r$ (being r the radius of the identified optic disc), as shown in the example of Figure 5(b), excluding sufficient region to guarantee the posterior analysis in the desired conditions.

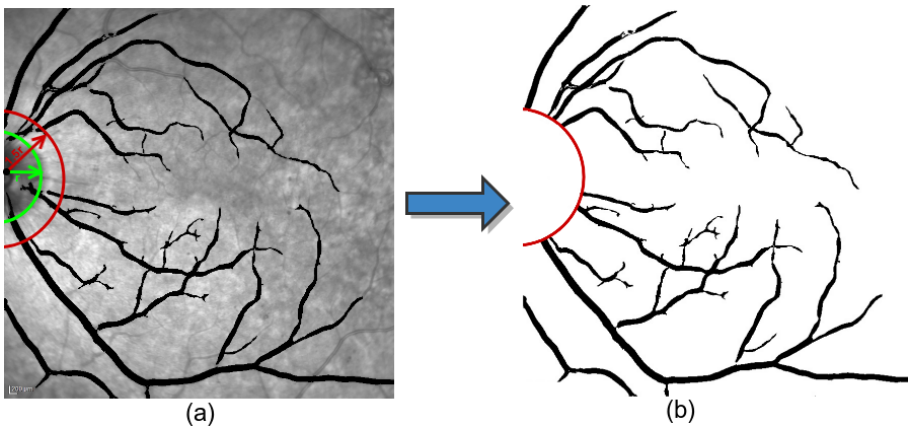

Fig. 5. Example of the optic disc location. (a) Optic disc detection, where r represents the radius of the optic disc and $1.5 \times r$ represents the brightness contiguous region to be removed. (b) Removal of the optic disc region in the segmented vasculature image.

2.3 Artery/Vein Vessel Classification

In this stage, we perform the automatic classification of the identified retinal vasculature into arteries and veins. To achieve this goal, we divide this stage into three constituent steps, as represented in Figure 6. These steps are herein progressively detailed.

Profile Extraction. Firstly, we obtain the vessel profiles in the original NIR retinography image, profiles that are posteriorly used in the process of the blood vessel classification. To achieved that, we based our strategy in the proposal of Vázquez *et al.* [20]. In particular, for each point P of the vessel centerlines, we obtain four equidistant vessel points P_i. These points are used as reference to obtain their corresponding perpendicular lines that are limited by both vessel edges. The vessel intensities over these perpendicular lines determine the vessel profile that is analysed to classify the referenced point, P. This strategy is applied over the entire vascular structure. Figure 7 shows a representative example of

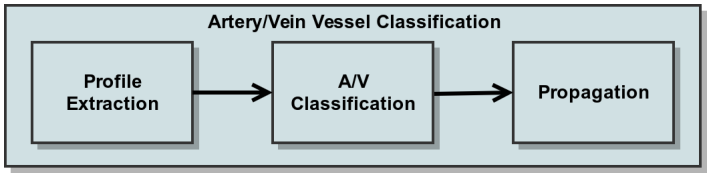

Fig. 6. Steps of the artery/vein vessel classification stage.

the vessel profile extraction, including the representation of the extraction of the perpendicular lines.

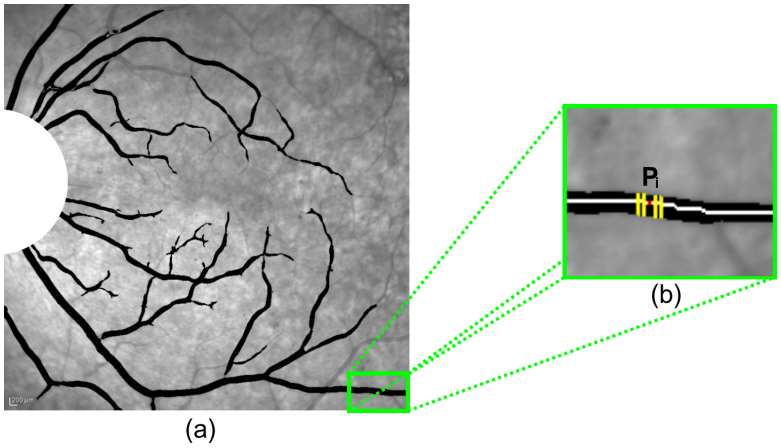

Fig. 7. Example of the vessel profile extraction. (a) Overlap between the result of the vessel segmentation and the NIR retinography image. (b) The four yellow lines, that are perpendicular to the vessel centerlines, identify the vessel profiles at the points that are posteriorly used in the classification process.

Artery/Vein Classification. In this second step, we use a machine learning approach to discriminate the retinal vessel tree between these two types. Normally, the arteries and veins are distinguished according to its branching pattern and morphology. In this work, the vectors of characteristics are obtained by means of the method proposed by Grisan *et al.* [31] that consist of two components:

- $\mu(H)$ (from HSL color space).
- $\sigma^2(R)$ (from RGB color space).

For the classification task, we selected the k-means clustering algorithm [32], given its simplicity and computational efficiency. This unsupervised learning

strategy was used to calculate the centroids for each of the two clusters using the feature vectors as input. As result of this approach, each vascular position of the vessel centerline is categorized as belonging to an artery or vein. In Figure 8, we explain the result of the classification method where the red points describe arteries whereas blue points indicated veins.

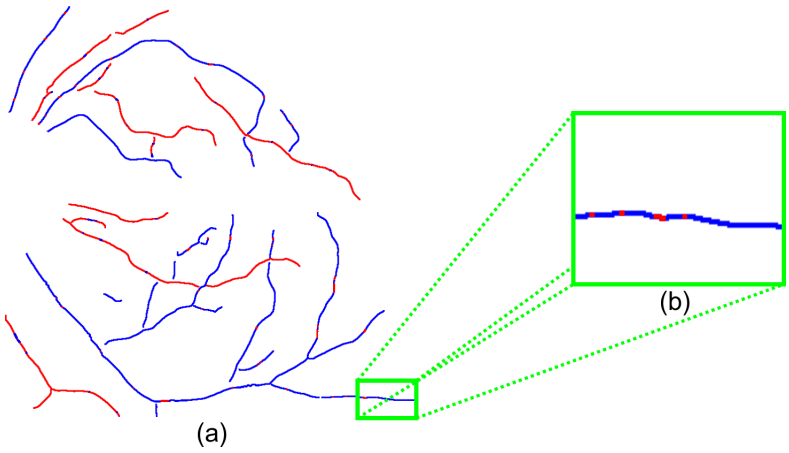

Fig. 8. Example of A/V classification. (a) Results of A/V classification in the entire vascular structure. (b) Red points represent arteries whereas blue points are veins.

Propagation. In the third and last step, a post-processing strategy is applied using the anatomical knowledge of the retinal vascular structure to identify and correct the possible misclassifications of the individual vessel points. Many times, the vascular points that belong to the same vascular segment can be classified into different categories (see Figure 9). This particular situation can be caused by possible changes in the brightness profiles, speckle noise or the presence of small capillaries, situations that are frequently present in this type of images and that typically produce these attenuations.

To decrease the influence of these misclassifications, using the context of the classifications, a voting process is carried out in the entire vascular segment. To achieve this, a voting process over each vascular segment is done. Then, the category with the higher number of votes is considered the winning class and, consequently, propagated to all the vessel points of the same vascular segment. In Figure 10, we can see a representative example of the final classification of the retinal vessels into arteries and veins after using the propagation step.

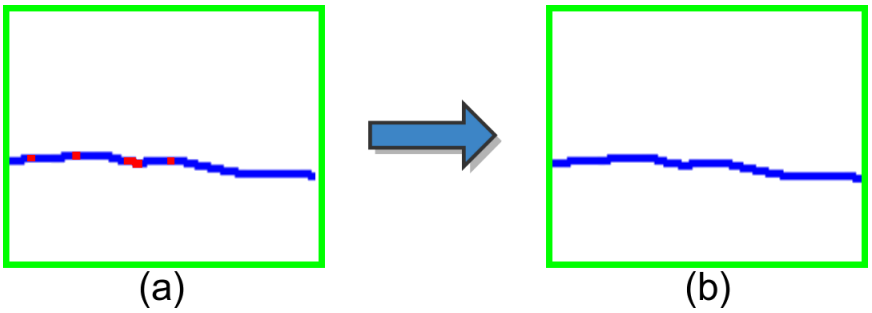

Fig. 9. Example of propagation of the winning class by a majority vote of all the points of the same vascular segment. (a) Vascular segment without propagation. (b) Vascular segment with propagation.

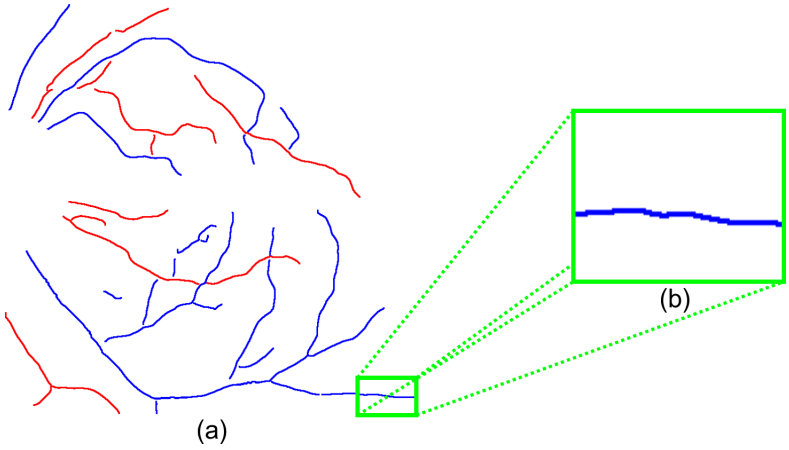

Fig. 10. Final result of the A/V classification stage. (a) Final result of the classification process with propagation applied to all the vascular segments. (b) Final result of a given vascular segment with propagation.

3 Results and Discussion

The proposed method was tested using a dataset of 30 OCT scans of different patients including their corresponding NIR retinography images. These images were taken with a confocal scanning laser ophthalmoscope Spectralis® OCT (Heidelberg Engineering). The OCT scans are centered on the macula, from both left and right eyes of healthy patients and presenting a high-resolution. The local ethics committee approved this study, which was conducted in accordance with the tenets of the Helsinki Declaration.

In order to test the performance of the proposed work, the OCT images were manually labelled by an expert clinician, identifying the arteries and veins. The dataset is composed by a total of 597 vascular segments. Next, this dataset was randomly divided in two subsets with the same size, one for training and the other for testing.

The proposed method was evaluated using the following metrics: Accuracy, Sensitivity and Specificity (Equations (2), (3) & (4), respectively). These measurements use as reference the true positives (TP), false positives (FP), true negatives (TN), and false negatives (FN) using the artery and vein classifications. In this work, we consider TPs as correctly identified arteries, whereas TNs as correctly identified veins.

$$\text{Accuracy} = \frac{TP + TN}{TP + FP + FN + TN} \tag{2}$$

$$\text{Sensitivity} = \frac{TP}{TP + FN} \tag{3}$$

$$\text{Specificity} = \frac{TN}{TN + FP} \tag{4}$$

Firstly, the classification system before the propagation step was evaluated over all the vessel points of the retinal vessel tree. Figure 11 shows the confusion matrix that is associated with the mentioned manual labelling of the expert clinician. Moreover, Table 2 summarises the performance of the proposed method. As we can see, the results provide a good balance between Accuracy, Sensitivity and Specificity (88.54%, 90.50% and 86.66%, respectively). We also have to consider that these OCT scans are normally taken over the macular region, as is the case of all the images of our dataset, region that normally contains smaller vessels in comparison with other parts of the eye fundus, reinforcing the analysis of the obtained performance. Additionally, a ROC curve was performed to compare the results of Sensitivity and Specificity, obtaining an Area Under the Curve (AUC) of 0.886 (see Figure 12).

Then, the classification approach that includes the propagation stage was evaluated in all the vessel coordinates that were included in the study. As mentioned, the propagation stage identifies and corrects the possible misclassifications of the vessels points in the same vascular segment. Table 2 presents the results of the comparative analysis through Accuracy, Sensitivity and Specificity

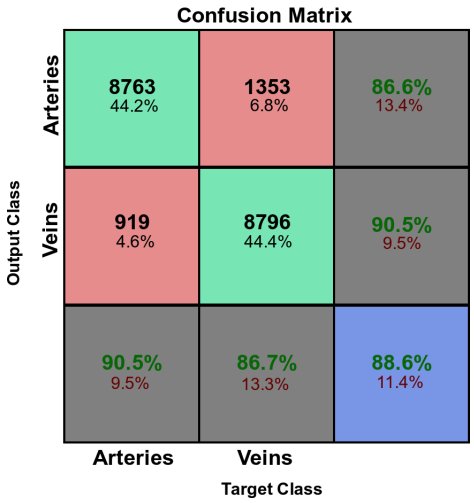

Fig. 11. Confusion matrix in the A/V classification process without propagation.

Table 1. Accuracy, specificity and sensitivity results in the A/V classification process without propagation.

Accuracy	Sensitivity	Specificity
88.54%	90.50%	86.66%

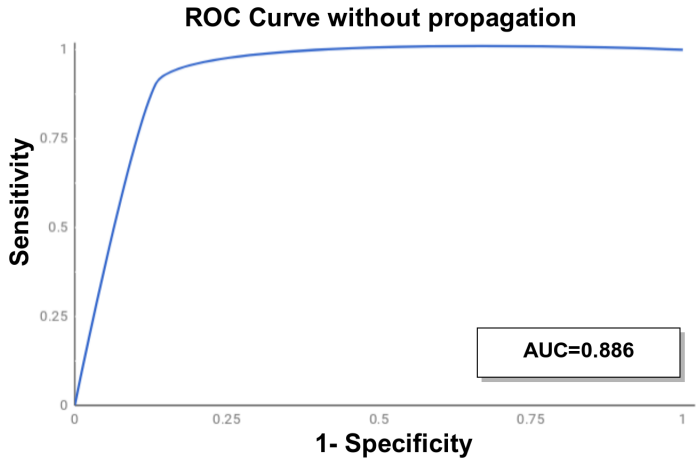

Fig. 12. ROC curve with the results of the classification process without propagation.

(90.10%, 91.67% and 88.59%, respectively). As we can see, the results from the proposed method including the propagation step are satisfactory. In addition, Figure 13 shows the ROC curve obtained by the proposed system, with an area under the curve of 0.901, reinforcing the validity of the designed methodology.

Table 2. Accuracy, specificity and sensitivity results in the A/V classification process with propagation.

Accuracy	**Sensitivity**	**Specificity**
90.10%	91.67%	88.59%

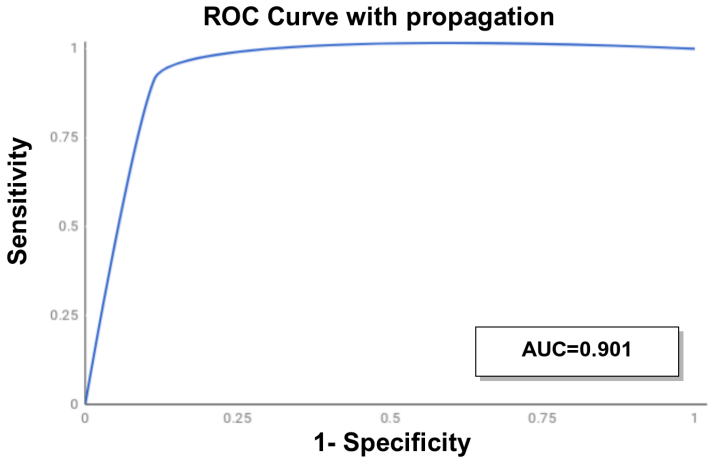

Fig. 13. ROC curve with the results of the classification process using propagation.

Despite the non-existence of any other proposal for the same image modality, we compared the proposed system with other reference approaches of the literature that were proposed for classical retinographies. The results of this comparison are shown in Figure 14. As we can see, our proposed method offers a competitive performance, outperforming the rest of the strategies, considering that each one was tested in their particular conditions and datasets.

Figure 15 shows a representative example illustrating the final result of the proposed methodology. As we can see, the method offers accurate results, providing information that can be easily analysed by the experts clinicians in their daily practice.

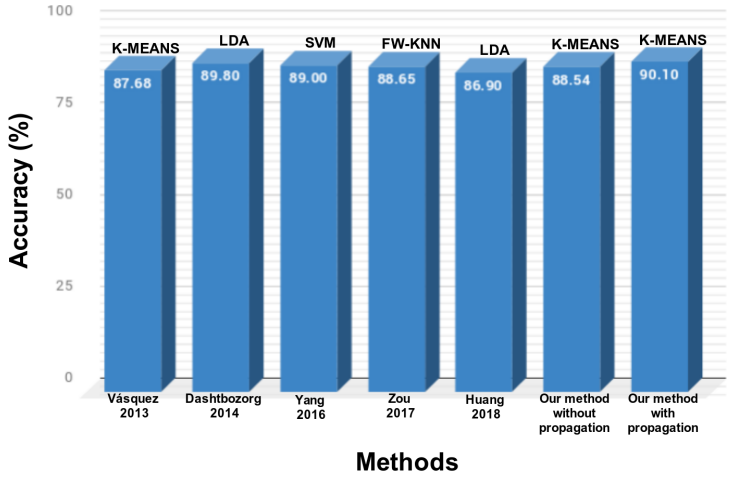

Fig. 14. Vessel classification performance comparative between different techniques of the literature and our proposal.

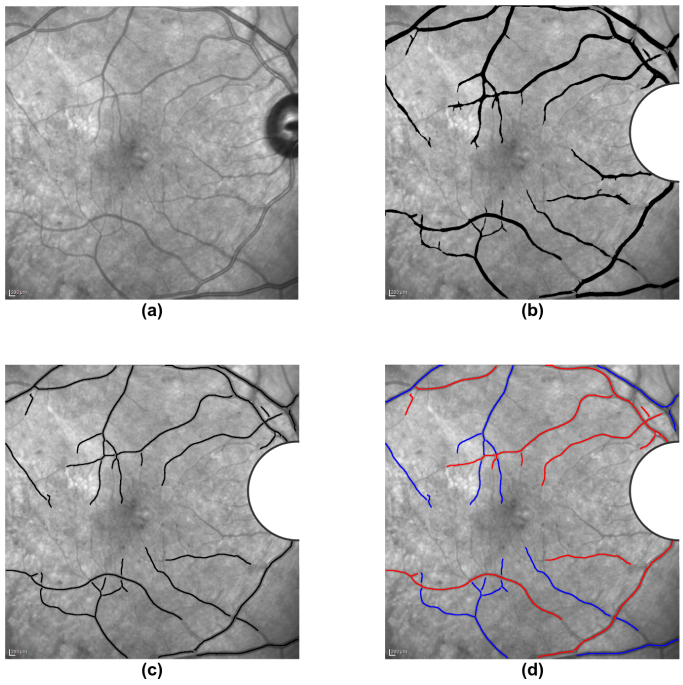

Fig. 15. Example of final result of the proposed methodology. (a) NIR retinography image. (b) Removal of the optic disc region and segmentation of the vasculature image. (c) Vessel tree centerline identification image. (d) Final result of the vascular segment with propagation.

4 Conclusions

The retina is the only tissue of the human body where the morphological information of the blood vessels can be directly obtained non-invasively and in vivo. A precise identification and characterization of the retinal vasculature and potential interesting biomarkers facilitate the diagnose, prevention and treatment of many systemic diseases, such as hypertension, diabetes or arteriosclerosis, among others, that significantly modify and damage the blood vessels architecture.

The CAD systems are increasing its relevance in the daily clinical practice, many of them also including the analysis of many medical image modalities, facilitating the doctor's analysis and diagnosis. Hence, these systems are developed to assist the clinical experts and simplify their work of detection and interpretation of characteristic pathological patterns that are typically present in the medical images of interest.

Among all the modalities, the OCT imaging is a non-invasive medical image modality with a high-speed capture process (being taken in real time) that provides a three-dimensional image of the biological tissues of the eye fundus with micron-level resolution. These specifications enable a precise evaluation and detection of slight modifications in the retinal microcirculation structure.

In this work, we present a new computerized system for the automatic retinal vasculature extraction and classification into arteries and veins using the NIR retinography images. These images are taken in combination with the histological sections in the OCT scans. To identify and classify the vessel structures, the proposed method analyzes the characteristics of each point of the vascular tree structure. The strategy combines the application of the k-means clustering technique with the feature vectors that were obtained from the extracted vessel profiles.

To validate the proposed methodology, we used 30 OCT scans of different patients including their corresponding NIR retinography images. From this OCT image dataset, 597 vessels were identified and manually label by an expert clinician. As result, the proposed method provided an accuracy of a 90.10% in the classification process. This satisfactory performance was achieved with the complete version of the method including the application of the propagation stage. Finally, we performed a comparative analysis with similar proposals that are present in the literature. This review emphasized the relevance and efficiency of the proposed method, comparatively with the rest of the approaches.

Although the favourable obtained results, we expect to reinforce the proposed methodology. In that sense, as future works, we aim to improve the different phases of the method to increase the success rates. In particular, we plan to extend the methodology with the inclusion of a more heterogeneous set of features as well as different testing classifiers to increase the performance of the method. Further, future plans include the design and implementation of an automatic method for the AVR calculation as a relevant biomarker, among others of interest. This way, we take the opportunity of having identified and categorized the arterio-venular tree to derive useful interesting biomarkers for being provided to the specialist. Finally, a CAD system could be developed to combine this

methodology with an automatic detection of other eye-related diseases, such as the diabetic retinopathy.

Acknowledgments This work is supported by the Instituto de Salud Carlos III, Government of Spain and FEDER funds of the European Union through the PI14/02161 and the DTS15/00153 research projects and by the Ministerio de Economía y Competitividad, Government of Spain through the DPI2015-69948-R research project. Also, this work has received financial support from the European Union (European Regional Development Fund - ERDF) and the Xunta de Galicia, Centro singular de investigación de Galicia accreditation 2016-2019, Ref. ED431G/01; and Grupos de Referencia Competitiva, Ref. ED431C 2016-047.

References

1. Anne Eichmann, Li Yuan, Delphine Moyon, Ferdinand Lenoble, Luc Pardanaud, and Christiane Breant. Vascular development: from precursor cells to branched arterial and venous networks. *International Journal of Developmental Biology*, 49(2-3):259–267, 2003.
2. Joaquim de Moura, Jorge Novo, Pablo Charlón, Noelia Barreira, and Marcos Ortega. Enhanced visualization of the retinal vasculature using depth information in oct. *Medical & biological engineering & computing*, 55(12):2209–2225, 2017.
3. Aljoscha S Neubauer, Matthias Luedtke, Christos Haritoglou, Siegfried Priglinger, and Anselm Kampik. Retinal vessel analysis reproducibility in assessing cardiovascular disease. *Optometry and Vision Science*, 85(4):E247–E254, 2008.
4. Thanh T Nguyen and Tien Yin Wong. Retinal vascular changes and diabetic retinopathy. *Current diabetes reports*, 9(4):277–283, 2009.
5. Ronald Klein, A Richey Sharrett, Barbara EK Klein, Lloyd E Chambless, Lawton S Cooper, Larry D Hubbard, and Greg Evans. Are retinal arteriolar abnormalities related to atherosclerosis?: The atherosclerosis risk in communities study. *Arteriosclerosis, thrombosis, and vascular biology*, 20(6):1644–1650, 2000.
6. Larry D Hubbard, Rosemary J Brothers, William N King, Limin X Clegg, Ronald Klein, Lawton S Cooper, A Richey Sharrett, Matthew D Davis, and Jianwen Cai. Methods for evaluation of retinal microvascular abnormalities associated with hypertension/sclerosis in the atherosclerosis risk in communities study1. *Ophthalmology*, 106(12):2269–2280, 1999.
7. Rupert RA Bourne, Seth R Flaxman, Tasanee Braithwaite, Maria V Cicinelli, Aditi Das, Jost B Jonas, Jill Keeffe, John H Kempen, Janet Leasher, Hans Limburg, et al. Magnitude, temporal trends, and projections of the global prevalence of blindness and distance and near vision impairment: a systematic review and meta-analysis. *The Lancet Global Health*, 5(9):e888–e897, 2017.
8. TJ MacGillivray, E Trucco, JR Cameron, Baljean Dhillon, JG Houston, and EJR Van Beek. Retinal imaging as a source of biomarkers for diagnosis, characterization and prognosis of chronic illness or long-term conditions. *The British journal of radiology*, 87(1040):20130832, 2014.
9. Muthu Rama Krishnan Mookiah, U Rajendra Acharya, Chua Kuang Chua, Choo Min Lim, EYK Ng, and Augustinus Laude. Computer-aided diagnosis of diabetic retinopathy: A review. *Computers in biology and medicine*, 43(12):2136–2155, 2013.

10. Jorge Novo, A Hermida, Marcos Ortega, Noelia Barreira, Manuel G Penedo, JE López, and C Calvo. Hydra: A web-based system for cardiovascular analysis, diagnosis and treatment. *Computer methods and programs in biomedicine*, 139:61–81, 2017.
11. Gabriela Samagaio, AiAda Estévez, Joaquim de Moura, Jorge Novo, Maria Isabel Fernandez, and Marcos Ortega. Automatic macular edema identification and characterization using oct images. *Computer Methods and Programs in Biomedicine*, 163:47–63, 2018.
12. D Tony Liu and X William Xu. A review of web-based product data management systems. *Computers in industry*, 44(3):251–262, 2001.
13. Maya Kalev-Landoy, Alexander C Day, M Francesca Cordeiro, and Clive Migdal. Optical coherence tomography in anterior segment imaging. *Acta Ophthalmologica*, 85(4):427–430, 2007.
14. Albert A Michelson and Edward W Morley. On the relative motion of the earth and of the luminiferous ether. *Sidereal Messenger, vol. 6, pp. 306-310*, 6:306–310, 1887.
15. Vinayak S Joshi, Joseph M Reinhardt, Mona K Garvin, and Michael D Abramoff. Automated method for identification and artery-venous classification of vessel trees in retinal vessel networks. *PloS one*, 9(2):e88061, 2014.
16. Behdad Dashtbozorg, Ana Maria Mendonça, and Aurélio Campilho. An automatic graph-based approach for artery/vein classification in retinal images. *IEEE Transactions on Image Processing*, 23(3):1073–1083, 2014.
17. Yi Yang, Wei Bu, Kuanquan Wang, Yalin Zheng, and Xiangqian Wu. Automated artery-vein classification in fundus color images. In *International Conference of Young Computer Scientists, Engineers and Educators*, pages 228–237, 2016.
18. Claudia Kondermann, Daniel Kondermann, and Michelle Yan. Blood vessel classification into arteries and veins in retinal images. In *Medical Imaging 2007: Image Processing*, volume 6512, page 651247, 2007.
19. D Relan, T MacGillivray, L Ballerini, and Emanuele Trucco. Retinal vessel classification: sorting arteries and veins. In *Engineering in Medicine and Biology Society (EMBC), 2013 35th Annual International Conference of the IEEE*, pages 7396–7399, 2013.
20. SG Vázquez, Brais Cancela, Noelia Barreira, Manuel G Penedo, M Rodríguez-Blanco, M Pena Seijo, G Coll de Tuero, Maria Antònia Barceló, and Marc Saez. Improving retinal artery and vein classification by means of a minimal path approach. *Machine vision and applications*, 24(5):919–930, 2013.
21. RA Welikala, PJ Foster, PH Whincup, AR Rudnicka, CG Owen, DP Strachan, SA Barman, et al. Automated arteriole and venule classification using deep learning for retinal images from the UK Biobank cohort. *Computers in biology and medicine*, 90:23–32, 2017.
22. Fantin Girard and Farida Cheriet. Artery/vein classification in fundus images using CNN and likelihood score propagation. In *Signal and Information Processing (GlobalSIP), 2017 IEEE Global Conference on*, pages 720–724, 2017.
23. Fan Huang, Behdad Dashtbozorg, and Bart M ter Haar Romeny. Artery/vein classification using reflection features in retina fundus images. *Machine Vision and Applications*, 29(1):23–34, 2018.
24. Bei-Ji Zou, Yao Chen, Cheng-Zhang Zhu, Zai-Liang Chen, and Zi-Qian Zhang. Supervised vessels classification based on feature selection. *Journal of Computer Science and Technology*, 32(6):1222–1230, 2017.

25. Joaquim de Moura, Jorge Novo, Marcos Ortega, Noelia Barreira, and Pablo Charlón. Artery/vein classification of blood vessel tree in retinal imaging. In *VISIGRAPP (4: VISAPP)*, pages 371–377, 2017.
26. David Calvo, Marcos Ortega, Manuel G Penedo, and Jose Rouco. Automatic detection and characterisation of retinal vessel tree bifurcations and crossovers in eye fundus images. *Computer methods and programs in biomedicine*, 103(1):28–38, 2011.
27. I Caderno, M Penedo, N Barreira, C Mariño, and F González. Precise detection and measurement of the retina vascular tree. *Pattern Recognition and Image Analysis*, 15(2):523, 2005.
28. Marianne Blanco, Manuel G Penedo, Noelia Barreira, Marta Penas, and María J Carreira. Localization and extraction of the optic disc using the fuzzy circular hough transform. In *International Conference on Artificial Intelligence and Soft Computing*, pages 712–721, 2006.
29. Josef Kittler. On the accuracy of the sobel edge detector. *Image and Vision Computing*, 1(1):37–42, 1983.
30. Karun P Philip, Edwin L Dove, David D McPherson, Nina L Gotteiner, William Stanford, and Krishnan B Chandran. The fuzzy hough transform-feature extraction in medical images. *IEEE Transactions on Medical Imaging*, 13(2):235–240, 1994.
31. Enrico Grisan and Alfredo Ruggeri. A divide et impera strategy for automatic classification of retinal vessels into arteries and veins. In *Engineering in medicine and biology society, 2003. Proceedings of the 25th annual international conference of the IEEE*, volume 1, pages 890–893, 2003.
32. James MacQueen et al. Some methods for classification and analysis of multivariate observations. In *Proceedings of the fifth Berkeley symposium on mathematical statistics and probability*, volume 1, pages 281–297, 1967.